2020-08-07

Grain size distribution and sedimentology in volcanic mass-wasting flows: implications for propagation and mobility

Makris, S

10.1007/s00531-020-01907-8
International Journal of Earth Sciences
Springer Science and Business Media LLC

Grain size distribution and sedimentology in volcanic mass-wasting flows: implications for propagation and mobility

Symeon Makris[1*], Irene Manzella[1], Paul Cole[1], Matteo Roverato[2]
[1]School of Geography, Earth and Environmental Science, University of Plymouth, Plymouth, UK
[2] Department of Earth Sciences, University of Geneva, Switzerland
*symeon.makris@plymouth.ac.uk

Abstract:

The sedimentological characteristics of mass-wasting flow deposits are important for assessing the differences between phenomena and their propagation and emplacement mechanisms. In the present study, nine volcanic debris avalanche deposits and eight lahar deposits are considered, from the literature. Their sedimentology is expressed in the descriptive statistics: median grain size, sand, gravel and finer particle proportion, skewness and sorting. Analysis of the data from the literature confirms that lahars and debris avalanches diverge in their grain size distribution and in their evolution during propagation. Comminution of particles due to interparticle interactions acts in debris avalanches, whereas debulking is enabled in lahars due to water saturation. The findings support previous studies suggesting that debris avalanches can be considered as dense granular flows where the effect of inertial collisions of solid fragments are more important than fluid effects. Therefore, grain size distribution characteristics, such as the percentage of large proportions of fine particles, remains a valid candidate factor for their high mobility.

Keywords: debris avalanche, runout, volcanic, lahar, grain size distribution

1. Introduction:

The long runout of large mass-wasting flows was first reported by Heim (1882) and have subsequently been further studied in diverse settings, even extraterrestrial, by several authors (including but not limited to: Hsü 1975; Davies 1982; Siebert 1984; Glicken 1991; Corominas 1996; Legros 2002; Hungr and Evans 2004; Davies and McSaveney 2012; Manzella and Labiouse 2013; van Wyk de Vries and Delcamp 2015). The mobility of both volcanic debris avalanches (VDA) and non-volcanic debris avalanches (DA) is far greater than what would be predicted by simple frictional models (Legros 2002). This is commonly expressed by small apparent coefficients of friction, expressed as the H/L ratio, initially introduced by Heim (1932), between elevation loss (H) and runout in the direction of flow (L) during propagation (Scheidegger 1973; Hsü 1975). This coefficient of friction is used in literature as a measure of mobility of VDAs and DAs (e.g. Shreve 1968; Erismann 1979). Simple frictional models would predict values of~0.5-0.6 for DAs and VDAs, however, they typically exhibit H/L values of 0.1-0.2 (see Figure 1 and table 2) (Scheidegger 1973; Hsü 1975; Davies 1982; Ui 1983; Legros 2002; Dufresne 2009). Although many theories have been proposed for the high mobility as presented in table 1 (for reviews, see Davies 1982; Erismann and Abele 2001; Hungr 2001; Legros 2002; Collins and Melosh 2003; Friedmann et al. 2006; Manzella and Labiouse 2008; Davies and McSaveney 2012), the issue is still controversial (Banton et al. 2009; Davies and McSaveney 2012). Models aiming to represent their propagation and emplacement need to express these long runouts, but at the same time be consistent with the sedimentological and geomorphological observations of their deposits (Dufresne 2009). Sedimentological observation-based studies have attempted to contribute to the understanding of the propagation and the internal processes of these flows by examining their grain size distributions (GSD) (e.g. Siebert et al. 1995, 2004; Glicken 1996; Roverato et al. 2011; Roverato and Capra 2013; Dufresne et al. 2016a; Bernard et al. 2017; Dufresne and Dunning 2017) and morphology of deposit (e.g. Ui 1983; Ui and Glicken 1986; Glicken 1991; Roverato et al. 2015; Dufresne et al. 2016b; Magnarini et al. 2019).

The term volcanic mass-wasting flow, in this study, refers to the propagation of volcanic material downslope under gravity. The term makes no distinction as to their water content and sediment concentration. The mass-wasting flows considered are VDAs and lahars. VDAs (as well as non-volcanic DAs) are extremely rapid flows of fragmented rock derived from a slope failure (Sharpe 1938; Schuster and Crandell 1984; Hungr 2001) or a volcanic flank collapse (Siebert 1984); and may evolve from an initial rockfall or rockslide (Hungr and Evans 2004; Clague and Stead 2013). Although they may contain water, VDAs are not water-saturated (Iverson 1997; Legros 2002) as the majority of pore spaces are occupied by air so that the mass is mostly supported by particle-to-particle interactions (Siebert et al. 2006; Vallance and Iverson 2015). Lahars are defined as rapidly-flowing, gravity-driven mixtures of rock, debris and water from a volcano (Vallance and Iverson 2015). Large quantities of unconsolidated material is required for their initiation (Lavigne and Thouret 2002). In contrast to VDAs, in lahars, the material is water-saturated with pore spaces filled with water (Iverson 1997; Scott et al. 2001; Legros 2002; Griswold and Iverson 2007). In the literature, lahars typically include sediment concentrations >60% by volume, whereas hyperconcentrated flows have sediment concentrations 20-60% (Fisher et al. 1984; Vallance 2000). Lahars can be closely associated with VDAs as they can evolve from the propagating VDA mass with the incorporation of water, or originate from the remobilisation of VDA deposits (VDAD) (Crandell 1971; Glicken 1991). However, even if they have a similar initial composition, they show fundamental differences in runouts and in the deposit characteristics; (Crandell 1971; Pierson and Scott 1985; Glicken 1991; Iverson 1997; Scott et al. 2001; Legros 2002; Vallance and Iverson 2015).

While water can affect VDA propagation as a lubricating or fluidising medium (Bagnold 1954; Voight et al. 1983, 1985; Legros 2002; Roverato et al. 2015); there are fundamental differences between not fully saturated or even dry VDAs and saturated lahars (Smyth 1991; Iverson 1997; Scott et al. 2001). However, the effect on propagation of both the water content and material differences are still unclear (Hürlimann and Ledesma 2000; Legros 2002).

Following the approach used by Dunning (2004), the present study analyses and compares the GSD of VDADs and lahar deposits and offers a comparison to allow the evaluation of the effect of water and the extent of its contribution to high mobility in VDAs, as well as revealing similarities or differences in the mode of propagation of the two mass-wasting flows.

2. Sedimentary characteristics of VDADs:

Material mobilised by different VDAs can be heterogeneous in origin and thus size and strength. However, there have been a number of studies regarding their sedimentology (e.g. Siebert 1984; Ui and Glicken 1986; Glicken 1991; Smyth 1991; Caballero and Capra 2011; Roverato et al. 2015); revealing some characteristic features:

1. Highly fragmented (jigsaw) sections of the source volcano, preserved as large blocks up to hundreds of meters in size (Glicken 1991), that nonetheless remain coherent and preserve initial outline (e.g. Ui and Glicken 1986; Ui 1989; Glicken 1991; Palmer et al. 1991; Tost et al. 2014). These are referred to as blocks or megablocks in the literature (Glicken 1991) and are not composed of one compact clast.
2. Formation of distinct facies within deposits (e.g. Ui and Glicken 1986; Glicken 1996; Belousov et al. 1999; Roverato et al. 2015).
3. Poor mixing of the incorporated lithologies and sedimentary units often leading to the preservation of original stratigraphy and areas of distinct lithologies within the deposit (e.g. Shreve 1968; Siebert 1984; Glicken 1996; Voight et al. 2002).
4. The GSD exhibits high heterogeneity throughout the deposits and even within the same facies (Glicken 1996; Bernard et al. 2008).

Due to the deposit heterogeneity and poor sorting, there is unlikely to be an average grain size distribution that could meaningfully characterise these deposits for inter-deposit comparison (Bernard et al. 2009), nonetheless, general trends can still be explored and give meaningful insights. What is typical is that the main interior of deposits with long runout is composed of fragmented debris produced by the fracturing, disaggregation and comminution of the original material (Roverato et al. 2015), and jigsaw-fractured but relatively coherent blocks (Shreve 1968; Glicken 1991). Their component parts are usually angular to very angular (Glicken 1991; Roverato et al. 2011). Source stratigraphy is locally retained despite long runout distances, and shear bands, faults, and block-in-matrix fabrics are common features (Siebert 1984; Glicken 1991; Davies and McSaveney 2009). The GSD of some VDADs have been reported to be bimodal (e.g. Mount St. Helens 1980 as shown in figure 7a) (Glicken 1996; Vallance 2000; Siebert 2002; Vallance and Iverson 2015). Other than these general features, lithology might have a major control on the GSD and sedimentology of the final deposits; as is the case in DAs (Dufresne et al., 2017) although there are large differences between volcanic and non-volcanic material. Significant differences in the material characteristics might, therefore, impact the mobility of VDAs.

In VDADs the main facies observed are:

1. Hummocky surface:
   The surface of VDADs displays a hummocky topography and longitudinal and transverse ridges (Siebert 1984; Glicken 1991; Bernard et al. 2008). Levees sometimes form on the sides of the flow, as is the case for the Mount St. Helens 1980 DAD (Voight et al. 1983) and Socompa (Francis et al. 1985). The surface hummocks in the topography of VDADs is a characteristic feature (Ui 1989). The size of the hummocks tends to decrease away from the axis of the deposit, however, their density increases towards the margins (Siebert 1984). The hummocks often, but not always, contain blocks, and some of them are only composed by one block (figure 2)(Siebert 1984).

The main body of VDADs is subdivided into the end member block facies and mixed facies (referred to as matrix facies in literature prior to Glicken 1991) (Ui 1983; Ui and Glicken 1986; Glicken 1991; Siebert et al. 1995).

2. <u>The mixed facies:</u>
   The mixed facies consists of brecciated debris of a mixture of rock types derived from different parts of the source volcano as well as juvenile material and material incorporated during propagation from the path (Ui 1989; Glicken 1991) forming a heterogeneous matrix of sand-silt grain sizes with few blocks (Bernard et al. 2008). Particle sizes range from micrometres to metres in size (Glicken 1991). The material

in this facies lacks sorting and stratification (Ui 1989). Laminations, stretched clasts and injections in cataclased blocks in the mixed facies indicate its motion during the propagation (Bernard et al. 2008).

3. The block facies:
The block facies is composed of coherent, but to some degree unconsolidated fragments (blocks) of the original volcanic body (figure 2) which might preserve original stratification, intrusive contacts or other features (Ui 1989). These blocks can be up to hundreds of meters in size (Glicken 1991) and are often partially deformed and faulted (Ui and Glicken 1986) to create the ''jigsaw cracks'' (figure 2) which are characteristic of VDADs (Siebert 1984; Glicken 1991). However, for typical metre-sized blocks, few clasts preserve their original texture (Glicken 1991). There are few interblock features such as incomplete mixture material (Bernard et al. 2008). Blocks greater than one metre in diameter are common in most VDADs, however, they are lacking from some, such as the VDADs of Mount St. Helens (Glicken 1996) and Chimborazo (Bernard et al. 2008).

The block and mixed facies are not horizontally continuous or homogenously distributed; but rather characterise the location of different lithologies, blocks, and matrix within the body of a VDAD. Thus they can be present in proximity to each other (figure 2). Both the mixed and the block facies are sometimes further divided into other more specific facies according to characteristics such as lithology in poly-lithological deposits (Glicken 1991; Bernard et al. 2008; Godoy et al. 2017).

In addition, VDADs exhibit shear zones (figure 2) with finer particles but with the same lithology as neighbouring megaclasts (Smyth 1991; Roverato et al. 2015; Roberti et al. 2017). The easier pulverisation of weak volcanic material like vesicular scoria is likely to encourage the formation of a sand-rich matrix as Roverato et al. (2015) suggest is the case for the Pungurehu VDA (Taranaki volcano). This fine matrix allows the formation of irregular shear zones. These are thought to 'act as corridors of shear accommodation' around more coherent domains that are less exposed to shear, thus dictating where particle disaggregation is concentrated and any present fluids are focused. The protected sections are consequently deposited as the observed block facies (Roverato et al. 2015).

3. Sedimentary characteristics of lahars:

Lahar deposits are characteristically flat-topped (Crandell 1971; Glicken 1991; Palmer et al. 1991). The marginal edges of the deposit grade into the substrate without forming steep slopes (Ui 1989). In terms of internal structure, lahar deposits are massive, compact and consist of very poorly sorted fragments of the original mass (Vallance and Iverson 2015). More dilute lahar deposits are more similar to fluvial sand and gravel deposits (Crandell 1971). Lahar deposits are very homogenous (Vallance 2000; Vallance and Iverson 2015), lacking fractures and fault surfaces (Ui 1989). This lack of internal features is a diagnostic characteristic along with an abundance of air spaces in their matrix (Crandell 1971; Vallance and Iverson 2015). They may contain structurally intact boulders (unfractured compact single clasts) surrounded by the finer-grained material, but not fractured blocks (Ui 1989). Lahar deposits can be graded, especially if less dense material like pumice is present, which are concentrated at the top to form a lower density carapace (Vallance 2000). Also, larger boulders are concentrated at the top of the deposit, contributing to the reverse-grading (e.g. Pierson and Scott 1985; Ui 1989; Saucedo et al. 2008). However, normal grading with coarse material at the base and finer at the top has also been observed, at least locally, in some lahars (e.g. Crandell 1971; Pierson and Scott 1985b; Vallance and Scott 1997; Saucedo et al. 2008).

4. Data sources and method

This study provides a semiquantitative assessment of the GSD of VDA and lahar deposits, through the examination of nine VDADs and eight lahar deposits through data assembled from published studies. These volcanic mass-wasting flows were selected because detailed studies of their sedimentology are available. All

the events present long runouts and low H/L ratios (table 2). Other case studies were also considered but could not be included as the desired statistical descriptors or the raw sedimentological data for their calculation were not available. For the Cotopaxi VDAD, raw sedimentological data were kindly provided directly by the authors (Vezzoli et al. 2017). Data included for VDADs are from both the mixed and the block facies and are labelled appropriately where fitting. The events, their authors and their properties are listed in table 2. Sample strategies and analyses vary in these studies since the examination of the evolution of GSD was not the original aim of the data collection campaigns of the published works, however, trends can be extracted for each event independently. In particular, events in Cotopaxi, Colima and Mount St. Helens are significant as, lahars and VDA are available representing different type of mass-wasting flows composed by similar material. The Cotopaxi lahar data are not used for longitudinal evolution analyses because they are all collected from the same location. In other cases, where a specific statistical descriptor is used that could not be obtained for some events, these events are not included in that specific analysis. It should also be noted that in the paper of Glicken (1996) describing the Mount St. Helens VDAD, the distances of the sampling sites from the source are overestimated by a factor of 1.6 throughout the paper (probably due to an error in conversion from miles to kilometres). This is evident by the location of the sampling sites on the map in plate 4 of that publication. This is mentioned so that the valuable findings of the study are correctly interpreted.

The parameters used for the characterisation of the deposits are the statistical descriptors: median grain size, sand, gravel and silt and clay particle fractions, skewness and sorting. Grain size fractions are chosen because comparison of their distribution and abundance can allow the evaluation of the comminution processes and any preferential comminution of size classes. The sizes of each class are defined according to the Wentworth (1922) classification. In particular, the sand range coincides with the size of interest for the fine material commonly used in relevant studies of VDA and lahars deposits (e.g. Scott, 1988; Vallance and Iverson, 2015). Inclusive graphic sorting (σ) and skewness (sk_1) of Folk (Folk and Ward 1957; Folk 1968) are used for all events except Shiveluch VDA (Belousov et al. 1999) and Acajutla VDA (Siebert et al. 2004), where they were not available. In these two cases, Inman (1952) statistics are used instead, which although might not be directly comparable, can still reveal trend within the same deposit. The sorting coefficient (σ) describes the range in size required to encompass a given majority of the population around the mean. A low sorting coefficient thus describes a population with little spread around the mean. A higher sorting coefficient indicates that the population is spread over a larger range of sizes. A verbal classification from very well sorted to extremely poorly sorted was introduced by Folk (1968) and is presented in table 3. Folk skewness (sk_1) measures the degree to which the population approaches symmetry, and (in contrast to Inman) includes a measure of the ''tail'' (material outside the mode of the distribution) of the population. Positive skewness describes populations with large proportions of fine material (fine-skewed) and a tail in the coarser range of sizes; and negative skewness the opposite (coarse-skewed). A skewness of zero would describe a symmetrical distribution. Higher values describe progressively more fine-skewed distributions. A verbal classification of skewness by Folk (1968) suggests sk_1 +0.1 to -0.1 as nearly symmetrical, -0.1 to -0.3, fine-skewed and -0.3 to -1.0 as strongly coarse-skewed, and the opposite for fine-skewed populations.

5. Results - Grain Size Analysis:

Median grain size

Comparison of both median grain sizes of VDADs and lahar deposits demonstrates that the average grain size for lahars is consistently lower than VDADs, after the most proximal (~5-6km) parts of the deposits (figure 3). The median grain size of lahars demonstrates a rapid decline at these initial stage, and then slowly becomes finer. Although there is some overlap, lahars are consistently at the finer-grained end of the overall population. In the Mount St. Helens VDAD and lahars originating from the same event and material, the grain size distribution of the lahars is always finer.

Analysis of the longitudinal evolution of the median grain size in VDADs show a constant grain size with no obvious trend. Lahars, on the other hand, show a fining (previously identified by Pierson and Scott 1985; Scott 1988) both individually as well as in the combined population in figure 3.

Silt and clay, sand and gravel particle content

With decrease in median grain size, there is a decrease of the gravel content of the mass, and an equivalent increase in the sand component, both in lahar and VDADs (figure 4 a and b). Conversely, there is only a minor increase of the silt and clay component in both lahars and VDADs (figure 4c). The silt and clay content only reaches percentages greater than 20% in a few very fine samples.

Sorting

The majority of both VDAD and lahar samples are very poorly sorted (σ= 2 to 4). Several VDAD samples are extremely poorly sorted (σ>4), and very few are poorly sorted only from the Rio Pita VDA (figure 5b). With decreasing grain size the sorting of lahars improves and thus a decrease of the sorting coefficient is observed (figure 5a). This implies that their GSD becomes more concentrated around the mean and is less spread in terms of the grain size range. For lahars, this trend is consistent in all the lahars where data was available. This trend is not exhibited by the VDADs (figure 5b).

Skewness

Skewness data for VDADs exhibits a consistent decrease of skewness from positive to negative with decreasing median grain size (figure 6b). This signifies that initially, coarser material composes the majority of the mass with the finer particles generating a 'tail' in the GSD. Progressively, comminution generates more fines that become the majority of the GSD; however, a significant coarse component is preserved as a tail. This evolution is common in all VDADs (figure 6b). In lahars, an evolution towards negative skewness is not consistent in all events examined (figure 6a), indicating that a coarse tail is not generated in the GSD.

6. Discussion:

VDAD

The GSD data for VDADs show that as the median grain size decreases, the sorting remains largely unaffected in the very poorly sorted range (figure 5c), skewness decreases and progressively becomes negative (figure 6b), and there is an exchange between the gravel and sand component with very little increase in finer particles (figure 4). The VDAD GSD evolution of the skewness from positive to negative, that has been previously identified by Dunning (2004), suggests that although progressive comminution reduces the size of the coarse gravel that is initially the majority of the material, a substantial amount of the coarse particles is preserved. This is confirmed by the GSD histograms of VDADs as presented in figure 7a that suggests that a coarse mode is preserved as a second mode develops in the sand size range with fining. This supports that there is preferential comminution of the finer grains because fragmentation of larger particles requires collision with grains of equal or larger size, assuming equal strength as previously proposed by Davies and McSaveney (2009). The lack of a trend in sorting is also in agreement as sorting which describes the spread of the data around the mean of the population cannot represent the two modes generated. This phenomenon is also supported by the experimental findings of Hörz et al. (1984) who observed the evolution of the GSD of a rock sample after repeated impacts that caused comminution to the original rock mass. The authors observed the evolution of their particle population from positive to negative skewness with more impacts and comminution; meaning that more fines were produced with time while coarser particles were preserved in the mass, in agreement with the data present study. The analogue experiments of Caballero et al. (2014) further explore this relationship in granular flows generally and suggest that while coarse particles develop small fractures, contributing sharp edges as fine particles to the overall population, medium-sized particles can develop through-fractures, thus contributing fines and depleting the medium-size range with their comminution. This results in the observed bimodality, as well as the peak in the GSD, observed for many of the deposits in correspondence of the sand-size range. The preference for further fragmentation of medium size particle into finer ones because they require less energy leads to the preservation of the larger particles throughout the length of DAD, which is also consistent with geomorphic observation (e.g. Glicken, 1996; Roverato et al., 2015). Roverato et al. (2018) suggest that in the case of the Cubilche DA, the matrix was

generated by the continuous disintegration of existing fractures into finer particles whereas coarse ones were preserved. Such facies development was also documented in non-volcanic DAs by Dufresne et al. (2016a), who identified this evolution from proximal to distal sample locations including the progressive fining of smaller clasts and preservation of large "survivor clasts". Also, in experiments of crushing granular materials, large sizes are always preserved and are never lost despite continued shearing and crushing (Lade et al. 1996; Einav 2007).

The combined data from the studies illustrate an exchange between the gravel and sand content of the samples as they become finer (median grain size), while there is only a minor increase in the silt and clay content (figure 4). Other studies also report high proportions of particles in this size range in volcaniclastic deposits of intermediate and silicic composition from different parts of the world (Glicken, 1996 and references therein); as well as the lack of silt grade material or finer observed in VDADs (Roverato et al. 2018). These offer support that the preferential fracturing and comminution stop when the particles reach a sand size (-1ϕ to 4ϕ). This is because in volcanic environments at this size they are often composed of a single crystals of plagioclase, amphibole, and pyroxene in the -1ϕ to 3ϕ range (Davies et al. 1978). Particles and fragments produced by comminution just larger than -1ϕ likely consist of more than one crystal and are thus more easily broken than individual crystals. Therefore, particles classified in the sand-size range are often preserved.

The GSD data also suggest an evolution towards negative skewness (figure 6b) and a bimodality is observed in GSD histograms as also recognised in literature (Ui and Glicken 1986; Siebert 2002)(figure 7a). Glicken (1996) states that the matrix facies of the Mount St. Helens VDAD is in most areas characterised by a bimodal distribution with the fine-grained peak in the histogram between -1ϕ and 3ϕ (gravel); and the maxima of this peak typically lying between 0ϕ and 2ϕ (sand). The Cubilche VDAD was divided into different lithological units for analysis by Roverato et al. (2018) and bimodal distributions are generally exhibited in all the units. The less fragmented sections exhibit the coarse mode between−8ϕ and−7ϕ (gravel), while the fine mode is between −3ϕ and −1ϕ (gravel). However, when also considering the interclast matrix, the highest percentage of the samples is gravel (−8ϕ to−2ϕ) and sand (−1ϕ and +4ϕ). The increase of the sand to generate a mode and bimodality in the GSD of the samples that have experienced more fragmentation agrees with the hypothesis that the propagating mass will progressively evolve towards a larger sand-sized component during propagation (Glicken 1996). As the interclast matrix experiences more shear, and therefore comminution, sand particles increase disproportionally to finer particles. The simultaneous increase in the sand-size component and preservation of the coarsest particles generates the bimodality in such deposits with the finer mode of the distribution in the sand-size range. The coarse mode is likely to be a function of the source material and lithology as the size of the larger clasts that will be preserved is likely to be a function of the original lithology. The observed negative skewness represents this preservation of a significant component of coarse particles as a tail to the population.

For the VDADs the longitudinal evolution of the median grain size appears to not follow a trend; even though progressive comminution of particles is typically observed and reported downslope along VDADs in the literature (e.g. Perinotto et al. 2015; Roverato et al. 2015) (figure 3). The record of this process will theoretically be the progressive grain size reduction, within each facies, with increasing distance from source (Dunning 2004). The lack of a trend might reflect the heterogeneity of the deposits and the fact that the sampling strategies were not designed to reveal this fining. Glicken (1996) interprets the lack of fining to signify the lack of major fracturing of the clasts progressively during transport, and that fracturing occurs mainly near the source. The author suggests that since the trend is not visible in the data, clast-to-clast collisions that resulted in fracturing must have not been a major occurrence during transport. This could also be the impact of a high water content filling pores, increasing pore pressure and limiting particle interactions. However, sampling each facies individually is necessary to confirm these hypothesis as also suggested by Dunning (2004), Dufresne (2016) and Dufresne and Dunning (2017). Moreover, bulldozing and incorporation of material along the flow path can interfere with these processes and affect the GSD, especially with samples from basal facies (Bernard et al. 2008) (although no samples from basal facies are included in this study).

Lahar deposits

312 The lahar GSD data from the literature presented show a decrease of the median grain size with propagation
313 distance and an improvement in the sorting of lahars with decreasing median gran size (figure 6a), as is also
314 reported by Pierson and Scott (1985b) and Scott (1988). This is perhaps easier for the sampling strategies to
315 expose because of the higher homogeneity of lahar deposits (Vallance 2000) owing to greater mixing during
316 propagation compared to VDADs (Pierson and Scott 1985; Glicken 1991; Siebert 2002). GSD histograms of
317 lahars illustrated in figure 7b and 8 show a progressive removal of the coarsest particles; a process described
318 by Pierson and Scott (1985). The deposition of the coarsest particles eliminates any initial bimodality in the
319 material if they were previously deposited by VDAs as illustrated in figure 8 with gradual loss of the bimodality
320 of the Toutle River N. Fork Lahar (Scott, 1988). This evidence suggests the process of debulking and progressive
321 deposition of the coarsest particles in the mass (Pierson and Scott 1985). Debulking is the process where as the
322 lahar becomes progressively more dilute, it becomes less capable to transport the coarsest particles which are
323 preferentially deposited, resulting in decreasing sediment concentrations, and median grain size with
324 propagation distance (Fisher et al. 1984; Pierson and Scott 1985; Vallance 2000). The water content increases
325 and sediment concentration decreases as lahars evolve from debris flow to a more hyperconcentrated flow
326 during propagation. And in the distal phases, they can approach more alluvial type processes (Vallance 2000).
327 Although there is abundant evidence of cataclasis in lahar deposits, debulking is the process more likely to be
328 responsible for the fining observed in their depositional phase when they become more dilute (Pierson and
329 Scott 1985; Vallance 2000). The improvement of sorting is the result of the narrowing of the distribution of the
330 histogram as the coarsest particles are removed. The improvement in sorting of the Mount St. Helens North
331 and South Fork, Toutle River lahars by the narrowing of the range of the GSD can be observed in figures 7b and
332 8 and described by Pierson and Scott (1985). However, Vallance and Iverson (2015) and Vallance (2000) report
333 that the bimodality can also be preserved in some sections of lahars.

334 The skewness of lahar GSD does not exhibit a trend (figure 6a). However, the content of gravel and sand show
335 an exchange between them, while there is little increase in finer particles (figure 4).

336

337 Comparison

338 Geomorphologically, lahars and their deposits display considerable differences to VDADs due to different
339 conditions and propagation processes generated mainly by the higher water content of lahars (Ui 1989; Smyth
340 1991; Iverson 1997; Scott et al. 2001; Siebert 2002). Saturated lahars involve strong turbulence and mixing of
341 the incorporated sediment (Pierson and Scott 1985; Glicken 1991; Siebert 2002). This results in more
342 homogeneous deposits where original stratigraphy is not preserved as recognised by Ui (1989) and Vallance
343 (2000).

344 As the material becomes finer in VDADs, skewness becomes progressively lower and shifts from positive to
345 negative, as coarse material is preserved in the mass to generate a bimodality. In lahars, histograms suggest a
346 progressive preferential removal of the coarsest range of the GSD histogram, as described by Pierson and Scott
347 (1985) and shown in figure 7b and 8, leading to an improvement in sorting (figure 5a) (Pierson and Scott 1985),
348 but not always generating an effect on skewness (figure 6a) as the data presented by this study suggest. The
349 observed patterns suggest that the process of debulking (Vallance 2000) is responsible for the fining and
350 reduction of median grain size observed in lahars. The coarsest particles are progressively preferentially
351 deposited (Pierson and Scott 1985) and the GSD becomes finer. The debulking of lahars is enabled because
352 pore spaces are filled with water which acts as the transportation medium for the sediment (Smyth 1991).

353 Conversely, in VDAs, preferential fracturing of the finer particles means that a coarse mode is preserved even
354 though the fine mode increases (figure 7a). This leads to the skewness becoming progressively more negative
355 (figure 7b). The preferential comminution of particles coarser than sand (and preservation of sand-sized
356 particles) (Davies et al. 1978), is evident by the lack of finer particles as the sand component increases (figure
357 4). Therefore, in VDAs, fining is a result of progressive comminution of particles in the mass.

358 The importance of the GSD and bimodality on mobility might not be as important in lahars because water has
359 a major role in lubricating the motion (Iverson 1997). Water is nearly incompressible compared to air and thus

when it fills intergranular spaces it reduces the frequency and intensity of collisions and thus energy dissipation (Glicken, 1996 and references therein). Therefore, saturated lahars with intergranular fluid pressure move more efficiently than dry flows and are capable of much greater runouts (Iverson 1997; Denlinger and Iverson 2001). Due to water saturation, both liquid and solid interactions influence lahar behaviour, which differentiates them from VDAs (Vallance and Iverson 2015).

Implications for the role of water:

Some of the lahar deposits and VDADs compared by the present study originated from the same material (table 2); meaning that water content is likely to be the principal difference between them (Iverson 1997; Scott et al. 2001; Legros 2002; Griswold and Iverson 2007). These cases exhibit significant divergence in GSD. The findings support that the fining of lahars is the result of debulking of coarser particles enabled by water saturation of the propagating mass (Vallance and Iverson 2015). In the case of VDADs, fining is due to the comminution of the material, with progressive fragmentation of finer particles that require less energy (Davies et al. 1978). This process suggests frequent particle-particle interactions with no interstitial fluid.

The ability of VDAs to achieve runouts longer than expected by simple frictional models has led many authors to speculate that a fluid might be the agent reducing the dissipation of friction in the propagating mass (Kent 1966; Shreve 1968; Voight et al. 1983; Voight and Sousa 1994; reviewed in Legros 2002). As a fluidising medium, water is much more effective than air because of its properties making it much more incompressible (Legros 2002). Although it is suggested that VDAs are often not dry, they are probably only partially saturated (Legros 2002). However, in the case of the Mount St. Helens VDA Voight et al. (1983) argue that water had an important effect on propagation. The water would have been available from the ice-capping of the volcano, and the cone which was water-saturated prior to the event. There was also evidence of the water content in the deposit, in the form of lahars being generated hours after the deposition (Janda et al. 1981) and kettle holes from post-depositional melting of ice blocks (Voight et al. 1981). Crandell et al. (1984) considered that water was also important for the propagation of Mount Shasta VDAs. Examining the Rio Pita VDA, Cotopaxi, Smyth (1991) suggest that the volcano would have had an extensive snow cover and was affected by a wet weather system at the time of the event. They support that the mass was at least partly water-saturated. Also, VDAs such as at Shiveluch volcano (Belousov et al. 1999), Acajutla (Santa Ana volcano) (Siebert et al. 2004), Pungarehu (Taranaki Volcano) (Roverato et al. 2015) and others are suggested to have included, or incorporated during propagation, significant amounts of water. Siebert (1984) supported that water is vital in weakening volcanic material and lubricating flow of VDAs. Interstitial water can potentially locally reduce friction of a granular mass by partly supporting a fraction of the weight of the particles (Bagnold 1954; Legros 2002). The potential increase of pressure gradient in the fluid (even locally) could lead to support of solid loads and increase fluidity (Legros 2002). Voight et al. (1983, 1985) suggest that interstitial fluids and steam from heated water can at least locally contribute to buoyant forces and that enhanced mobility may be enhanced by the pressurized fluid-particle interactions.

However, in VDAs water is not present in quantities that enable it to become the transporting medium, as in lahars; or for complete fluidisation (Siebert 1984). As suggested by Smyth (1991) and by findings of the present study, water might have an impact on the mobility of VDA but is not the principal factor influencing propagation as is the case in lahars. In addition, present results showing the lack of debulking in VDAs suggest that water content is not sufficient to enable it and therefore that water does not become the transportation medium as it is in lahars. This confirms that particle to particle interactions as a leading role in the dynamics of VDAs.

7. Conclusion:

The present study carries out a semiquantitative assessment of the sedimentology of nine VDA and eight lahar deposits. The sedimentology is not only important for the original mass, but the evolution of the

sedimentology during propagation and emplacement can also provide evidence for the mechanisms and factors that allow high mobility.

The decrease in median grain size of lahars is the result of debulking and progressive deposition of the coarsest particles. This is reflected in improved sorting due to the narrowing of the GSD (figure 5a) which can also be observed in the evolution of GSD histograms (figure 8b and 9). Debulking is a process that is enabled because lahars are water-saturated and water is the transportation medium. In this case, particle to particle interactions are not as important for the evolution of the GSD as they are for VDAs.

In fact, data analysed here, suggest that particle to particle interactions in VDA propagating are responsible for comminution due to fracturing, in agreement also with the findings of the authors of the considered studies. Results show as well that preferential comminution happens within the finer particles where less energy is required. When sand-sized particles are reached though, comminution stops and particles are preserved because they are often composed of single crystals (Davies et al. 1978). The combination of these processes leads to progressively more negative skewness (figure 6b) and a bimodality developing in the GSD, with the finer mode composed of sand-sized particles as supported by geomorphic observations (Glicken 1996; Roverato et al. 2018). In addition, data show no evidence of debulking in VDAs confirming that the propagation mechanisms differ.

Although water content in VDAs can possibly play a role in their propagation, present results on their GSD distribution characteristics confirm that they can be considered as dense granular masses where the effects of inertial collision of solid fragments are more important than fluid effects and that particle to particle interactions are the main factor influencing the mobility of non-saturated mass wasting flows.

Acknowledgements

We would like to thank Dr Luigina Vezzoli for the e-mail communication kindly providing additional data on the published studies. We would also like to thank Dr Lorenzo Borselli and an anonymous reviewer for their in-depth review and comments that considerably improved this paper.

Figure Captions:

Figure 1: Apparent coefficient of friction (H/L) versus volume for continental VDAs, VDAs on volcanic islands, non-volcanic DAs and extraterrestrial DAs (modified from Hürlimann and Ledesma 2000; van Wyk de Vries and Delcamp 2015).

Figure 2: Schematic representation of debris avalanche deposit (modified after Roverato et al. 2015; Dufresne et al. 2016; Bernard et al. 2008).

Figure 3: Figure 3 Evolution of the grain size distribution of VDAs and lahars with propagation distance. Note that the x-axis is inverted so that size increases up the axis.

Figure 4: The evolution of specific grain size range component of the mass with decreasing median grain size: a. gravel, b. sand, c. silt and clay.

Figure 5: Median grain size versus sorting for: a. lahars, and b. VDAs (MF: mixed facies, BF: block facies, I: Indicates where Inman (Inman 1952) statistics were used; in all other cases Folk and Ward (Folk and Ward 1957; Folk 1968) statistics are used.

Figure 6: Median grain size versus skewness for: a. lahars, and b. debris avalanches (MF: mixed facies, BF: block facies).

Figure 7: Grain size distributions from: a. Mount St. Helens 1980 VDA (Glicken 1996), and b. South Fork Toutle River Lahar (Scott 1988). Data are from different locations indicated by the distance from the source (in km) at the top left of each plot.

Figure 8: Grain size distribution histograms from the North Fork Lahar (Scott 1988). Data are from different locations indicated by the distance from the vent (in km) at the top of each plot.

453 **Tables:**

454 *Table 1 Mechanisms proposed for the mobility of long runout landslides (adapted from Smyth, 1991)*

Mechanism Proposed	Author
Flow	Hsu 1975
Sliding	Ui 1985
Fluid-absent	
Highly energetic collisions among individual grains maintaining the original kinetic energy	Heim 1932
Acoustic/vibratory fluidisation – high-frequency vibration which momentarily relieves overburden pressure locally, allowing sliding to occur in the unloaded regions	Melosh 1979
Dry acoustically and seismically fluidised flow	Francis and Wells 1988
Spreading of a rapid granular mass	Davies 1982
Dynamic rock fragmentation	Davies and McSaveney 2002
Air lubricated or fluidised	
Trapped layer of compressed air beneath the mass, supporting it	Shreve 1968
Fluidisation by air: dilated upward flow of air within the mass maintains a low coefficient of friction **between particles**	Kent 1966; Wilson 1981 1948
Lubricated or fluidised by the presence of a fluid	
Water-saturated slide	Katayama 1974
Small amounts of water in the basal layer accommodating shear in a **wet basal zone** with reduced friction	Goguel 1978; Johnson 1978; Voight & Sousa 1994
High-pressure steam generated by frictional heat at the base of the flow	Goguel 1978
Highly energetic interstitial dust acting as intergranular fluid	Hsu 1975
A layer of molten rock generated at the base by frictional heat	Erissmann 1979
Gravitational sliding fractured and mobility enhanced by steam explosions	Ui 1983
Boiling of interstitial fluid by frictional heat - vaporised in the mass	Voight et al. 1983; Habib 1975
Specific to volcanic environments	
Volcanic gases injected along the slip plane	Prostka 1978
Hydrothermal fluids - allowing incomplete fluidisation of weak rocks	Siebert 1984
Fluidisation by volcanic gases	Voight et al. 1983
Magmatic Blast	Gorschkov & Dubik 1970
Fluidisation by hydrothermal and magmatic blast	Smyth and Clapperton 1986

455

456

457 *Table 2 Events considered in the present study. Note that some are related either geographically (bold, enclosed in thicker border), or both geographically and temporally (same shade colour).*

Type	Location	Sampling	Age	Runout	Volume	Water content	H/L	Source
DA	Pungarehu, Taranaki Volcano, NZ	several samples from each locality to cover all lithofacies, 13km length covered	25 ka	>27km	>7 km^3	incorporated snow, ice and substantial groundwater	<0.09	*Roverato et al. 2015*
DA	Shiveluch Volcano, Kamchatka, RS	samples from block facies, 10km length covered	multiple DADs	>15km	1.5 km^3	high	0.133	*Belousov et al. 1999; Hayashi and Self 1992*
DA	Cubilche, EC	outcrops few and concentrated	>30 ka	>20km	>3–3.5 km^3	initial low content <10%, increasing during propagation	0.063	*Roverato et al. 2018*
DA	San Marcos, Colima, MX	sampled along the deposit	>28 ka	22.55km	~1.3 km^3	<10%		Roverato and Capra 2013
DA	Tonila, Colima, MX	sampled along the deposit	15–16 ka	23.01km	~1 km^3	high		
Lahar	Montegrande ravine, Colima, MX	sampled along the deposit	15/09/2012					*Vàzquez et al. 2014*
DA	Acajutla, Santa Ana Volcano, SV	sampled along the deposit	<57 ka	~50 km	16 ± 5 km^3	very high - some areas classified as a cohesive debris flow	>0.05	*Siebert et al. 2004*
DA	Rio Pita, Cotopaxi, EC		4 ka	21km	2.1 km^3	local partial saturation	0.12	*Smyth 1991*
DA	**Cotopaxi**, EC	data from different facies in the same area	4.5 ka	20km	~2 km^3	not significant		*Vezzoli et al. 2017*
Lahar	Chillos Valley, **Cotopaxi**, EC **(evolved from Cotopaxi DA)**	sampled along northern and southern flow paths		326km	3.8 km^3	melted icecap saturated the material to generate the lahar		*Mothes et al. 1998*
Lahar	**Cotopaxi**, EC	one sample location, samples from different events	multiple, post-1150 AD			water released from summit glaciers with different mechanisms		*Pistolesi et al. 2013*
DA	**Mount St. Helens**, USA	sampled along the deposit, different facies	18/05/1980	29km	2.9 km^3	0.31 km^3, 11%	0.106	*Glicken 1996*
Lahar	Toutle River, North Fork, **Mount St. Helens (evolved from Mount St. Helens DA)**	sampled along the deposit						*Scott 1988*
Lahar	Toutle River, South Fork, **Mount St. Helens (evolved from Mount St. Helens DA)**							
Lahar	Toutle River, **Mount St. Helens**, USA	sampled along the deposit	19/03/1982	83km		Eruption of the volcano released a flood of water from the cater, $4x10^6 m^3$	0.06	*Pierson and Scott 1985*
Lahar	Popocatépetl, MX	sampled along the deposit	2001	>15km	2.3 $x10^5 m^3$	<25%		*Capra et al. 2004*
		sampled along the deposit	1997		4 $x10^5 m^3$			

458

459 *Table 3 Sorting classification (Folk 1968)*

Sorting Value (ϕ)	Sorting classification
0.00 - 0.35	very well sorted
0.35 - 0.50	well sorted
0.50 - 0.71	moderately well sorted
0.71 - 1.00	moderately sorted
1.00 - 2.00	poorly sorted
2.00 - 4.00	very poorly sorted
>4.00	extremely poorly sorted

460 **References:**

461 Bagnold RA (1954) Experiments on a gravity-free dispersion of large solid spheres in a Newtonian fluid under
462 shear. Proc R Soc London Ser A Math Phys Sci 225:49–63. https://doi.org/10.1098/rspa.1954.0186
463 Banton J, Villard P, Jongmans D, Scavia C (2009) Two-dimensional discrete element models of debris
464 avalanches: Parameterization and the reproducibility of experimental results. J Geophys Res Earth Surf
465 114:1–15. https://doi.org/10.1029/2008JF001161
466 Belousov A, Belousova M, Voight B (1999) Multiple edifice failures, debris avalanches and associated eruptions
467 in the Holocene history of Shiveluch volcano, Kamchatka, Russia. Bull Volcanol 61:324–342.
468 https://doi.org/10.1007/s004450050300
469 Bernard B, van Wyk de Vries B, Barba D, et al (2008) The Chimborazo sector collapse and debris avalanche:
470 Deposit characteristics as evidence of emplacement mechanisms. J Volcanol Geotherm Res 176:36–43.
471 https://doi.org/10.1016/j.jvolgeores.2008.03.012
472 Bernard B, Van Wyk de Vries B, Leyrit H (2009) Distinguishing volcanic debris avalanche deposits from their
473 reworked products: The perrier sequence (French Massif Central). Bull Volcanol 71:1041–1056.
474 https://doi.org/10.1007/s00445-009-0285-7
475 Bernard K, Thouret JC, van Wyk de Vries B (2017) Emplacement and transformations of volcanic debris
476 avalanches-A case study at El Misti volcano, Peru. J Volcanol Geotherm Res 340:68–91.
477 https://doi.org/10.1016/j.jvolgeores.2017.04.009
478 Caballero L, Capra L (2011) Textural analysis of particles from El Zaguán debris avalanche deposit, Nevado de
479 Toluca volcano, Mexico: Evidence of flow behavior during emplacement. J Volcanol Geotherm Res
480 200:75–82. https://doi.org/10.1016/j.jvolgeores.2010.12.003
481 Caballero L, Sarocchi D, Soto E, Borselli L (2014) Rheological changes induced by clastfragmentation in
482 debrisflows. J Geophys Res Earth Surf 119:1800–1817. https://doi.org/10.1002/2013JF002871.Received
483 Clague JJ, Stead D (2013) Landslides: Types, Mechanisms and Modleing
484 Collins GS, Melosh HJ (2003) Acoustic fluidization and the extraordinary mobility of sturzstroms. J Geophys Res
485 Solid Earth 108:1–14. https://doi.org/10.1029/2003jb002465
486 Corominas J (1996) The angle of reach as a mobility ındex for small and large landslides
487 Crandell DR (1971) Postglacial lahars from Mount Rainier Volcano, Washington. U S Geol Surv Prof Pap 667:80
488 Crandell DR, Miller CD, Glicken HX, et al (1984) Catastrophic debris avalanche from ancestral Mount Shasta
489 volcano, California. Geology 12:143–146. https://doi.org/10.1130/0091-
490 7613(1984)12<143:CDAFAM>2.0.CO;2
491 Davies DK, Quearry MW, Bonis SB (1978) Glowing avalanches from the 1974 eruption of the volcano Fuego,
492 Guatemala. Bull Geol Soc Am 89:369–384. https://doi.org/10.1130/0016-
493 7606(1978)89<369:GAFTEO>2.0.CO;2
494 Davies T, McSaveney M (2012) Mobility of long-runout rock avalanches. Landslides–types, Mech Model Ed by
495 JJ Clague D Stead 50–58
496 Davies TR, McSaveney MJ (2009) The role of rock fragmentation in the motion of large landslides. Eng Geol
497 109:67–79. https://doi.org/10.1016/j.enggeo.2008.11.004
498 Davies TRH (1982) Spreading of rock avalanche debris by mechanical fluidization. Rock Mech 24:9–24
499 Denlinger RP, Iverson RM (2001) Flow of variably fluidized granular masses across three-dimensional terrain: 2.
500 Numerical predictions and experimental tests. J Geophys Res Solid Earth 106:537–552.
501 https://doi.org/10.1029/2000JB900329
502 Dufresne A (2009) Influence of runout path material on rock and debris avalanche mobility : field evidence and
503 analogue modelling . Sci York 268
504 Dufresne A, Bösmeier A, Prager C (2016a) Sedimentology of rock avalanche deposits – Case study and review.
505 Earth-Science Rev 163:234–259. https://doi.org/10.1016/j.earscirev.2016.10.002
506 Dufresne A, Dunning S (2017) Process dependence of grain size distributions in rock avalanche deposits.
507 Landslides 14:1555–1563. https://doi.org/10.1007/s10346-017-0806-y
508 Dufresne A, Geertsema M, Shugar DH, et al (2017) Sedimentology and geomorphology of a large tsunamigenic
509 landslide, Taan Fiord, Alaska. Sediment Geol 364:302–318.
510 https://doi.org/10.1016/j.sedgeo.2017.10.004
511 Dufresne A, Prager C, Bösmeier A (2016b) Insights into rock avalanche emplacement processes from detailed
512 morpho-lithological studies of the Tschirgant deposit (Tyrol, Austria). Earth Surf Process Landforms
513 41:587–602. https://doi.org/10.1002/esp.3847
514 Dunning SA (2004) Rock Avalanches in High Mountains. PhD Thesis
515 Einav I (2007) Breakage mechanics-Part II: Modelling granular materials. J Mech Phys Solids 55:1298–1320.

https://doi.org/10.1016/j.jmps.2006.11.004
Erismann TH (1979) Mechanisms of large landslides. Rock Mech Felsmechanik Mécanique des Roches. https://doi.org/10.1007/BF01241087
Erismann TH, Abele G (2001) Dynamics of Rockslides and Rockfalls. Springer Science & Business Media
Fisher R V., Schmincke H-U, Fisher R V., Schmincke H-U (1984) Lahars. In: Pyroclastic Rocks. Springer Berlin Heidelberg, pp 297–311
Folk RL (1968) Petrologie of sedimentary rocks. Hemphll Publ Company, Austin 170. https://doi.org/10.1017/CBO9781107415324.004
Folk RL, Ward WC (1957) Brazos River Bar: A study in the significance of grain size parameters. J Sediment Petrol 27:3–26
Francis PW, Gardeweg M, Ramirez CF, Rothery DA (1985) Catastrophic debris avalanche deposit of Socompa volcano, northern Chile. Geology 13:600–603. https://doi.org/10.1130/0091-7613(1985)13<600:CDADOS>2.0.CO;2
Friedmann SJ, Taberlet N, Losert W (2006) Rock-avalanche dynamics: Insights from granular physics experiments. Int J Earth Sci 95:911–919. https://doi.org/10.1007/s00531-006-0067-9
Glicken H (1991) Sedimentary architecture of large volcanic-debris avalanches. In: Sedimentation in Volcanic Settings. pp 99–106
Glicken H (1996) Rockslide-debris avalanche of May 18, 1980, Mount St. Helens volcano, Washington. USGS Open File Report 96-677. Bull Surv
Godoy B, Rodríguez I, Pizarro M, Rivera G (2017) Geomorphology, lithofacies, and block characteristics to determine the origin, and mobility, of a debris avalanche deposit at Apacheta-Aguilucho Volcanic Complex (AAVC), northern Chile. J Volcanol Geotherm Res 347:136–148. https://doi.org/10.1016/j.jvolgeores.2017.09.008
Griswold JP, Iverson RM (2007) Mobility Statistics and Automated Hazard Mapping for Debris Flows and Rock Avalanches Scientific Investigations Report 2007 – 5276. USGS Sci Investig Rep 2007–5276:62
Hörz F, Cintala MJ, See TH, et al (1984) Grain size evolution and fractionation trends in an experimental regolith. J Geophys Res 89:C183. https://doi.org/10.1029/jb089is01p0c183
Hsü KJ (1975) Catastrophic debris streams (sturzstroms) generated by rockfalls. Bull Geol Soc Am. https://doi.org/10.1130/0016-7606(1975)86<129:CDSSGB>2.0.CO;2
Hungr O (2001) Rock avalanche motion
Hungr O, Evans SG (2004) Entrainment of debris in rock avalanches: An analysis of a long run-out mechanism. Bull Geol Soc Am 116:1240–1252. https://doi.org/10.1130/B25362.1
Hürlimann M, Ledesma A (2000) Giant Mass Movements in Volcanic Islands : the Case of Tenerife. 1–11
Inman D (1952) Measures for Describing the Size Distribution of Sediments. SEPM J Sediment Res. https://doi.org/10.1306/d42694db-2b26-11d7-8648000102c1865d
Iverson RM (1997) The physics of debris flows. Rev Geophys 35:245–296. https://doi.org/10.1029/97RG00426
Janda RJ, Scott KM, Nolan M, Martinson H (1981) Lahar movement, effects, and deposits. In: Lipman PW, D.R. M (eds) The 1980 Eruption of Mount St. Helens, Washington, 1250th edn. U.S. Geol. Surv., Prof. Pap., pp 461–478
Kent PE (1966) The Transport Mechanism in Catastrophic Rock Falls. J Geol 74:79–83
Lade P V., Yamamuro JA, Bopp PA (1996) Significance of particle crushing in granular materials. J Geotech Eng 122:309–316. https://doi.org/10.1061/(ASCE)0733-9410(1996)122
Lavigne F, Thouret JC (2002) Sediment transportation and deposition by rain-triggered lahars at Merapi Volcano, Central Java, Indonesia. Geomorphology 49:45–69. https://doi.org/10.1016/S0169-555X(02)00160-5
Legros F (2002) The mobility of long-runout landslides. Eng Geol 63:301–331. https://doi.org/10.1016/S0013-7952(01)00090-4
Magnarini G, Mitchell TM, Grindrod PM, et al (2019) Longitudinal ridges imparted by high-speed granular flow mechanisms in martian landslides. Nat Commun 10:1–7. https://doi.org/10.1038/s41467-019-12734-0
Manzella I, Labiouse V (2008) Qualitative analysis of rock avalanches propagation by means of physical modelling of non-constrained gravel flows. Rock Mech Rock Eng 41:133–151. https://doi.org/10.1007/s00603-007-0134-y
Manzella I, Labiouse V (2013) Empirical and analytical analyses of laboratory granular flows to investigate rock avalanche propagation. Landslides 10:23–36. https://doi.org/10.1007/s10346-011-0313-5
Palmer B, Alloway B, Vincent N (1991) Volcanic-Debris-Avalanche Deposits in New Zealand—Lithofacies Organization in Unconfined, Wet-Avalanche Flows. Sediment Volcan Settings 89–98. https://doi.org/10.2110/pec.91.45.0089

573 Perinotto H, Schneider JL, Bachèlery P, et al (2015) The extreme mobility of debris avalanches: A new model of
574 transport mechanism. J Geophys Res Solid Earth. https://doi.org/10.1002/2015JB011994
575 Pierson TC, Scott KM (1985) Downstream Dilution of a Lahar: Transition From Debris Flow to
576 Hyperconcentrated Streamflow. Water Resour Res 21:1511–1524.
577 https://doi.org/10.1029/WR021i010p01511
578 Roberti G, Friele P, van Wyk de Vries B, et al (2017) Rheological evolution of the mount meager 2010 debris
579 avalanche, southwestern british columbia. Geosphere 13:1–22. https://doi.org/10.1130/GES01389.1
580 Roverato M, Capra L (2013) Características microtexturales como indicadores del transporte y emplazamiento
581 de dos depósitos de avalancha de escombros del Volcán de Colima (México).pdf. 512–525
582 Roverato M, Capra L, Sulpizio R, Norini G (2011) Stratigraphic reconstruction of two debris avalanche deposits
583 at Colima Volcano (Mexico): Insights into pre-failure conditions and climate influence. J Volcanol
584 Geotherm Res 207:33–46. https://doi.org/10.1016/j.jvolgeores.2011.07.003
585 Roverato M, Cronin S, Procter J, Capra L (2015) Textural features as indicators of debris avalanche transport
586 and emplacement, Taranaki volcano. Bull Geol Soc Am 127:3–18. https://doi.org/10.1130/B30946.1
587 Roverato M, Larrea P, Casado I, et al (2018) Characterization of the Cubilche debris avalanche deposit, a
588 controversial case from the northern Andes, Ecuador. J Volcanol Geotherm Res.
589 https://doi.org/10.1016/j.jvolgeores.2018.07.006
590 Saucedo R, Macías JL, Sarocchi D, et al (2008) The rain-triggered Atenquique volcaniclastic debris flow of
591 October 16, 1955 at Nevado de Colima Volcano, Mexico. J Volcanol Geotherm Res 173:69–83.
592 https://doi.org/10.1016/j.jvolgeores.2007.12.045
593 Scheidegger AE (1973) On the prediction of the reach and velocity of catastrophic landslides. Rock Mech
594 Felsmechanik Mécanique des Roches 5:231–236. https://doi.org/10.1007/BF01301796
595 Schuster RL, Crandell DR (1984) No Title. Fourth Int Symp Landslides Proc Toronto 1:567–572
596 Scott K, Macias JL, Naranjo JA, et al (2001) Catastrophic debris flows transformed from landslides in volcanic
597 terrains: Mobility, hazard assessment, and mitigation strategies
598 Scott KM (1988) Origins, behavior, and sedimentology of lahars and lahar-runout flows in the Toutle-Cowlitz
599 River system. U S Geol Surv Prof Pap 74. https://doi.org/-
600 Sharpe CFS (1938) Landslides and related phenomena: a study of mass movement of soil and rock. Columbia
601 Uni Press New York 136pp.
602 Shreve RL (1968) The Blackhawk Landslide. Geol Soc Am Spec Pap 108:
603 Siebert L (1984) Large volcanic debris avalanches: Characteristics of source areas, deposits, and associated
604 eruptions. J Volcanol Geotherm Res 22:163–197. https://doi.org/10.1016/0377-0273(84)90002-7
605 Siebert L (2002) Landslides resulting from structural failure of volcanoes. GSA Rev Eng Geol 15:209–235.
606 https://doi.org/10.1130/REG15-p209
607 Siebert L, Alvarado GE, Vallance JW, Van Wyk De Vries B (2006) Large-volume volcanic edifi ce failures in
608 Central America and associated hazards. Spec Pap Geol Soc Am 412:1–26.
609 https://doi.org/10.1130/2006.2412(01)
610 Siebert L, Begét JE, Glicken H (1995) The 1883 and late-prehistoric eruptions of Augustine volcano, Alaska. J
611 Volcanol Geotherm Res 66:367–395. https://doi.org/10.1016/0377-0273(94)00069-S
612 Siebert L, Kimberly P, Pullinger CR (2004) The voluminous Acajutla debris avalanche from Santa Ana volcano,
613 western El Salvador, and comparison with other Central American edifice-failure events. Spec Pap Geol
614 Soc Am 375:5–23. https://doi.org/10.1130/0-8137-2375-2.5
615 Smyth M-A (1991) Movement and emplacement mechanisms of the Rio Pita Volcanic Debris Avalanche and its
616 role in the evolution of Cotopaxi Volcano. Aberdeen Univ Thesis, Ph D
617 Tost M, Cronin SJ, Procter JN (2014) Transport and emplacement mechanisms of channelised long-runout
618 debris avalanches, Ruapehu volcano, New Zealand. Bull Volcanol 76:1–14.
619 https://doi.org/10.1007/s00445-014-0881-z
620 Ui T (1989) Discrimination Between Debris Avalanches and Other Volcaniclastic Deposits. 201–209.
621 https://doi.org/10.1007/978-3-642-73759-6_13
622 Ui T (1983) Volcanic dry avalanche deposits - Identification and comparison with nonvolcanic debris stream
623 deposits. J Volcanol Geotherm Res 18:135–150. https://doi.org/10.1016/0377-0273(83)90006-9
624 Ui T, Glicken H (1986) Internal structural variations in a debris-avalanche deposit from ancestral Mount Shasta,
625 California, USA. Bull Volcanol 48:189–194. https://doi.org/10.1007/BF01087673
626 Vallance JW (2000) Lahars. Encycl volcanoes 601–616
627 Vallance JW, Iverson RM (2015) Lahars and Their Deposits, Second Edi. Elsevier
628 Vallance JW, Scott KM (1997) The Osceola Mudflow from Mount Rainier: Sedimentology and hazard
629 implications of a huge clay-rich debris flow. Bull Geol Soc Am. https://doi.org/10.1130/0016-

630 7606(1997)109<0143:TOMFMR>2.3.CO;2
631 van Wyk de Vries B, Delcamp A (2015) Volcanic Debris Avalanches. Elsevier Inc.
632 Vezzoli L, Apuani T, Corazzato C, Uttini A (2017) Geological and geotechnical characterization of the debris
633 avalanche and pyroclastic deposits of Cotopaxi Volcano (Ecuador). A contribute to instability-related
634 hazard studies. J Volcanol Geotherm Res 332:51–70. https://doi.org/10.1016/j.jvolgeores.2017.01.004
635 Voight B, Glicken H, Janda RJ, Douglass M (1981) Catastrophic rockslide avalanche of May 18 (Mount St.
636 Helens). US Geol Surv Prof Pap 1250:347–377
637 Voight B, Janda RJ, Glicken H, Douglass PM (1983) Nature and mechanics of the Mount St Helens rockslide-
638 avalanche of 18 May 1980. Geotechnique 33:243–273. https://doi.org/10.1680/geot.1983.33.3.243
639 Voight B, Janda RJ, Glicken H, Douglass PM (1985) Reply to Mr Skermer, in Discussion of Voight et al. (1983).
640 Geotechnique 35:362–369
641 Voight B, Komorowski JC, Norton GE, et al (2002) The 26 December (Boxing Day) 1997 sector collapse and
642 debris avalanche at Soufrière Hills Volcano, Montserrat. Geol Soc Mem 21:363–407.
643 https://doi.org/10.1144/GSL.MEM.2002.021.01.17
644 Voight B, Sousa J (1994) Lessons from Ontake-san: A comparative analysis of debris avalanche dynamics. Eng
645 Geol 38:261–297. https://doi.org/10.1016/0013-7952(94)90042-6
646 Wentworth CK (1922) A Scale of Grade and Class Terms for Clastic Sediments. J Geol 30:377–392.
647 https://doi.org/10.1086/622910
648
649

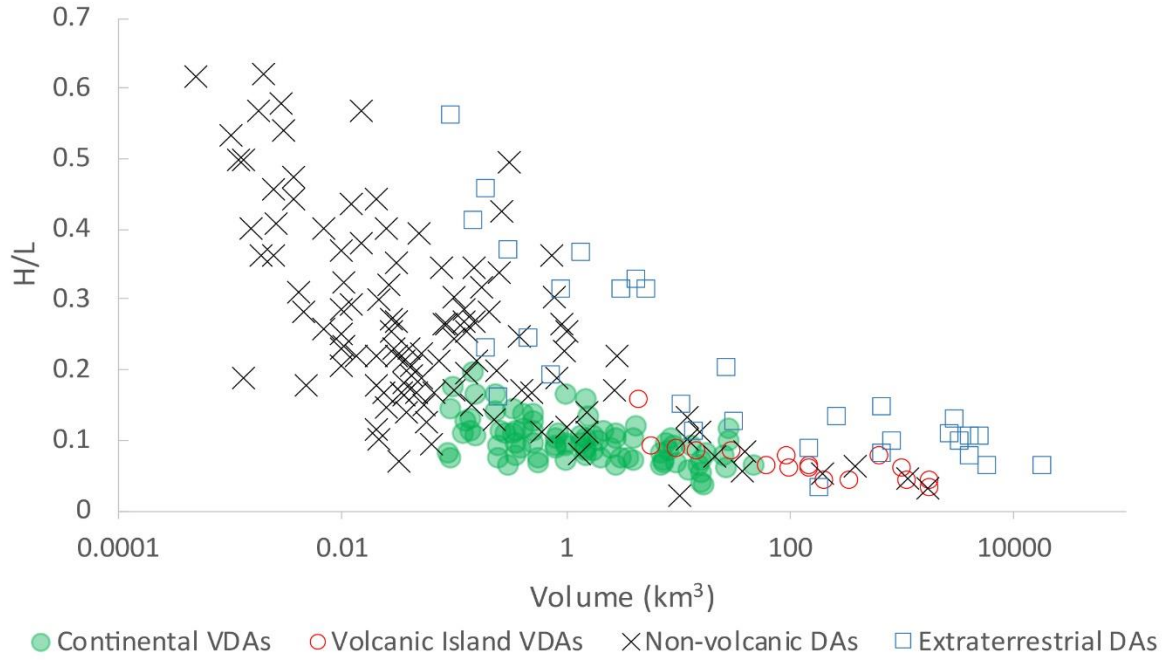

Figure 1

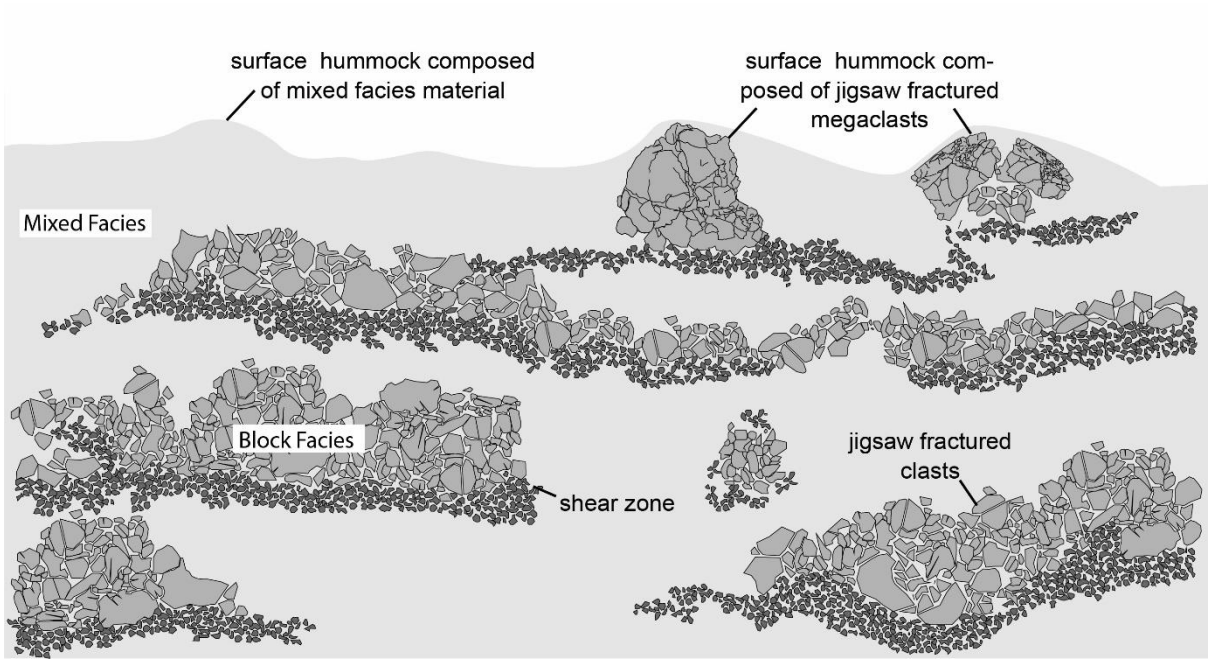

Figure 2

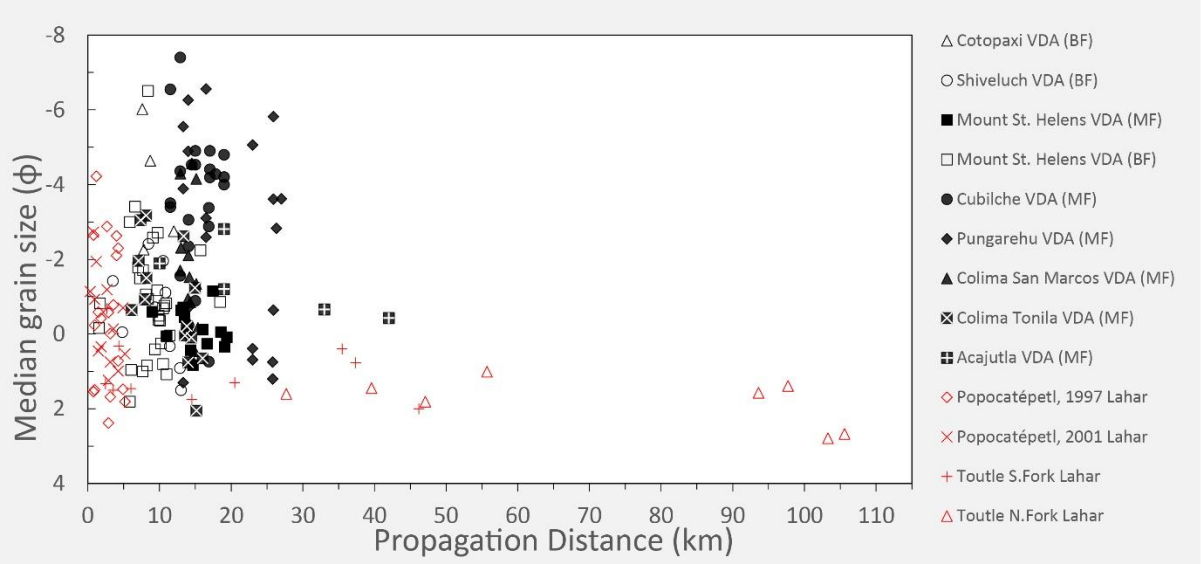

654

655 *Figure 3*

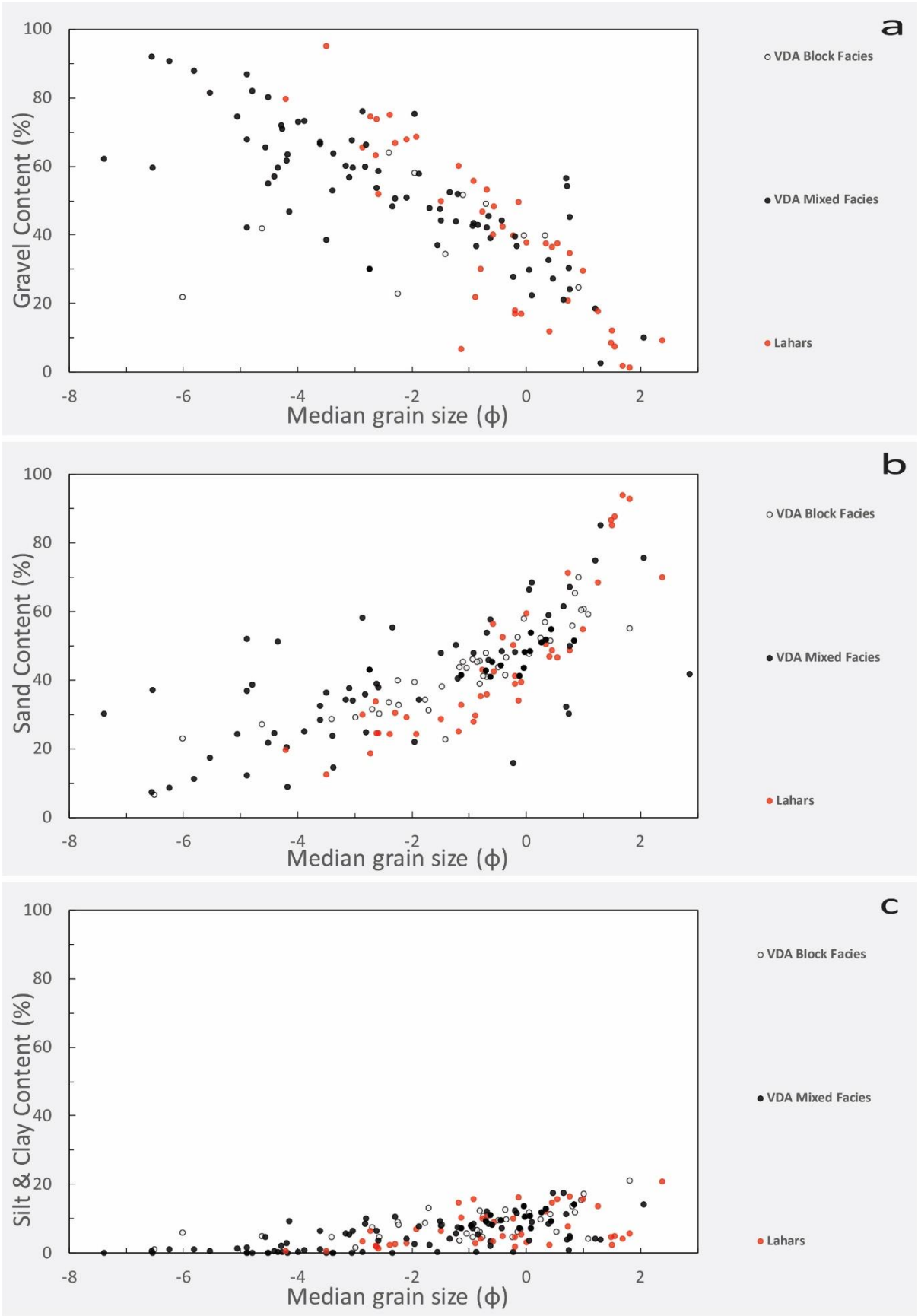

656

657 *Figure 4*

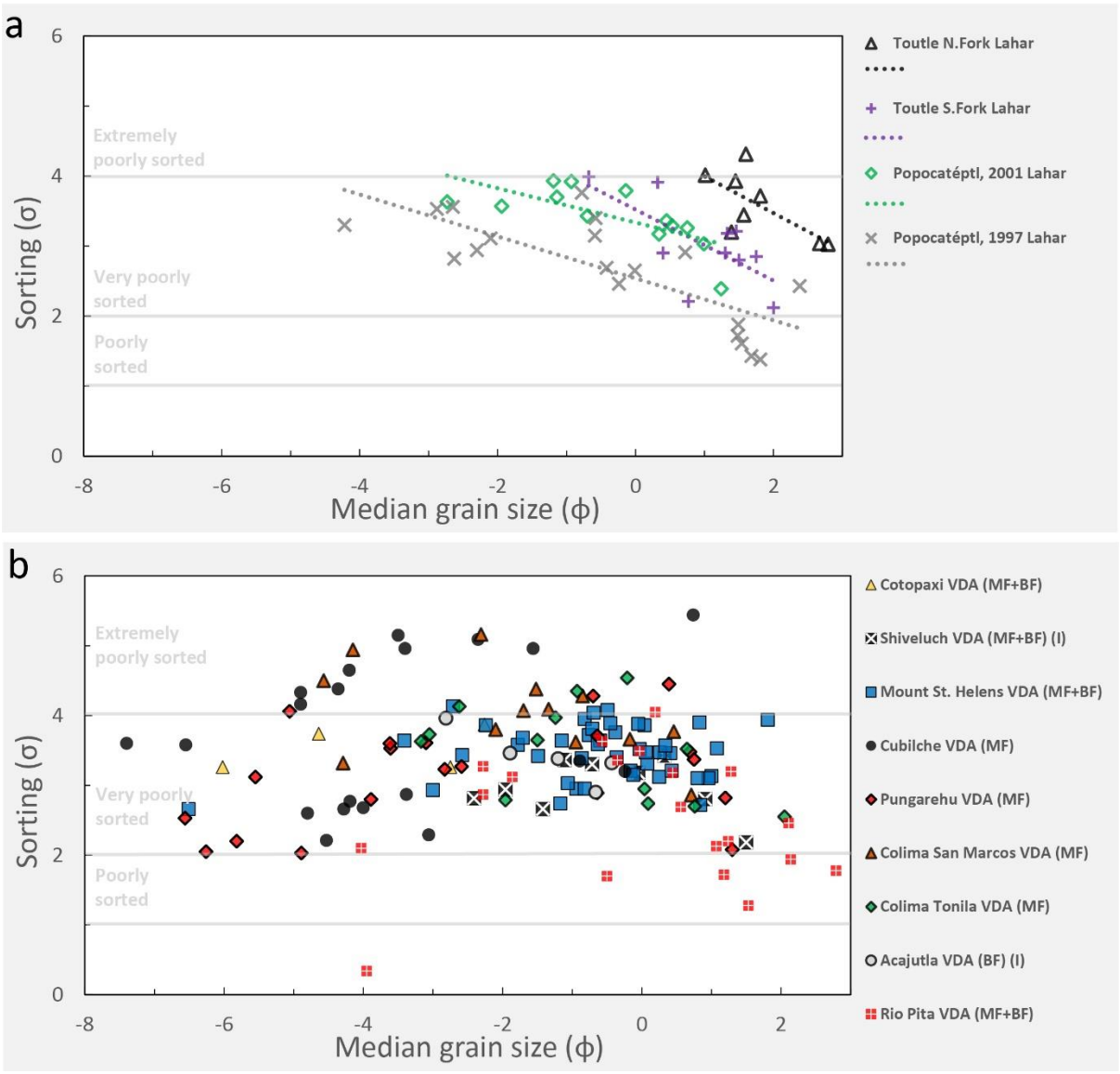
a
Sorting (σ)
Median grain size (ϕ)
Extremely poorly sorted
Very poorly sorted
Poorly sorted
Toutle N.Fork Lahar
Toutle S.Fork Lahar
Popocatéptl, 2001 Lahar
Popocatéptl, 1997 Lahar
b
Sorting (σ)
Median grain size (ϕ)
Extremely poorly sorted
Very poorly sorted
Poorly sorted
Cotopaxi VDA (MF+BF)
Shiveluch VDA (MF+BF) (I)
Mount St. Helens VDA (MF+BF)
Cubilche VDA (MF)
Pungarehu VDA (MF)
Colima San Marcos VDA (MF)
Colima Tonila VDA (MF)
Acajutla VDA (BF) (I)
Rio Pita VDA (MF+BF)

Figure 5

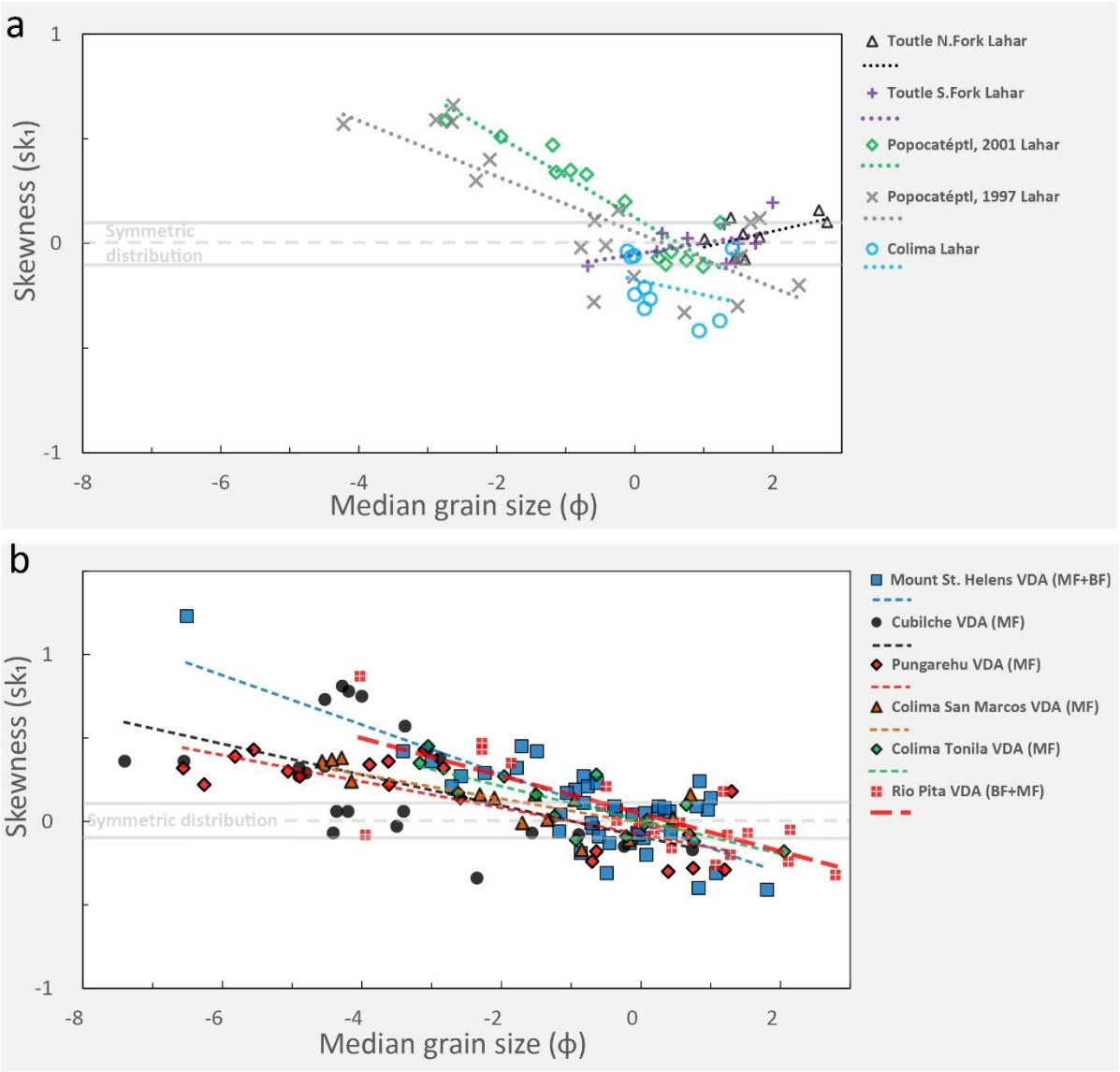
a
Skewness (sk1)
Median grain size (ϕ)
Symmetric distribution
Toutle N.Fork Lahar
Toutle S.Fork Lahar
Popocatéptl, 2001 Lahar
Popocatéptl, 1997 Lahar
Colima Lahar
b
Skewness (sk1)
Median grain size (ϕ)
Symmetric distribution
Mount St. Helens VDA (MF+BF)
Cubilche VDA (MF)
Pungarehu VDA (MF)
Colima San Marcos VDA (MF)
Colima Tonila VDA (MF)
Rio Pita VDA (BF+MF)

Figure 6

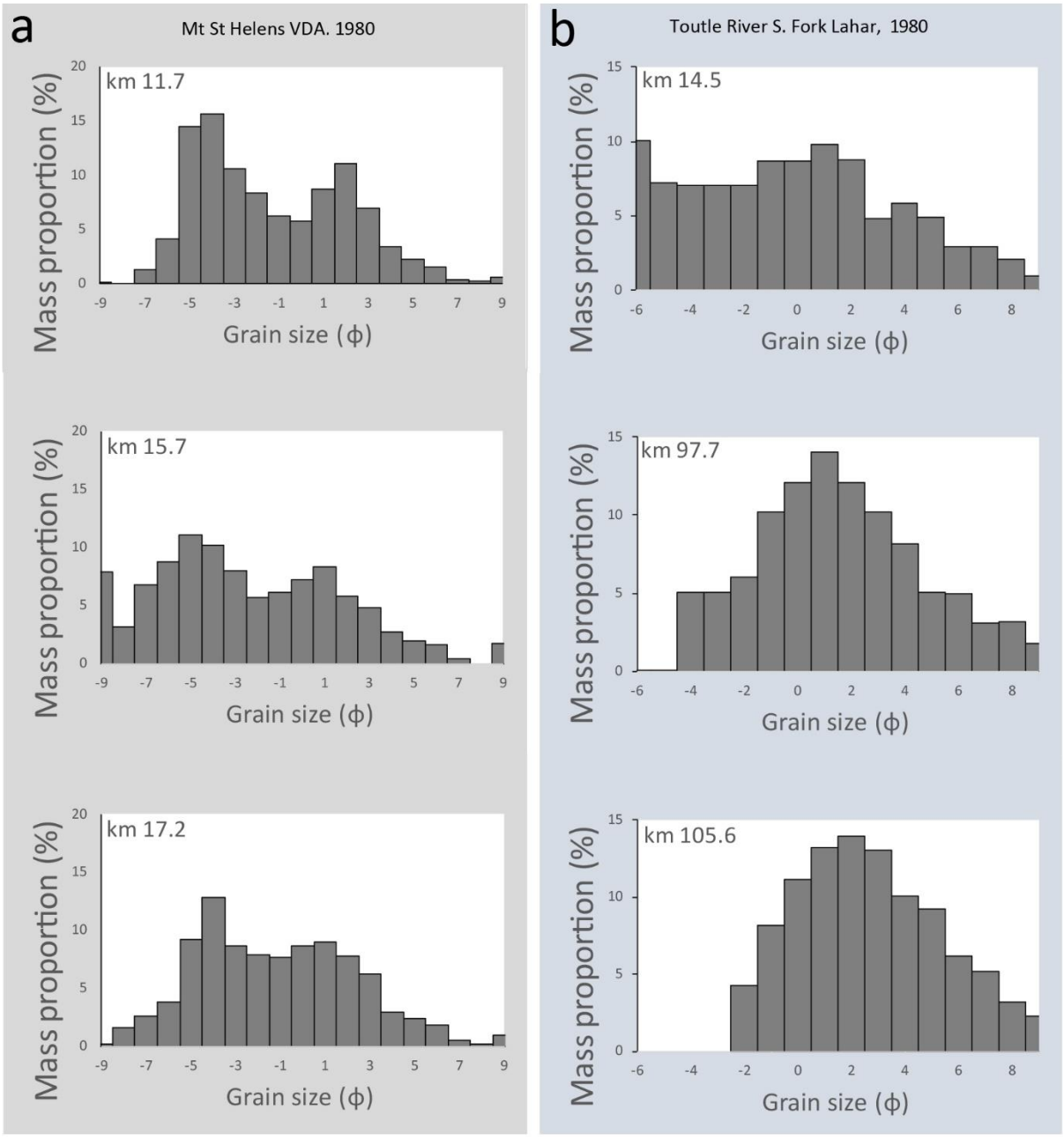

662

663 *Figure 7*

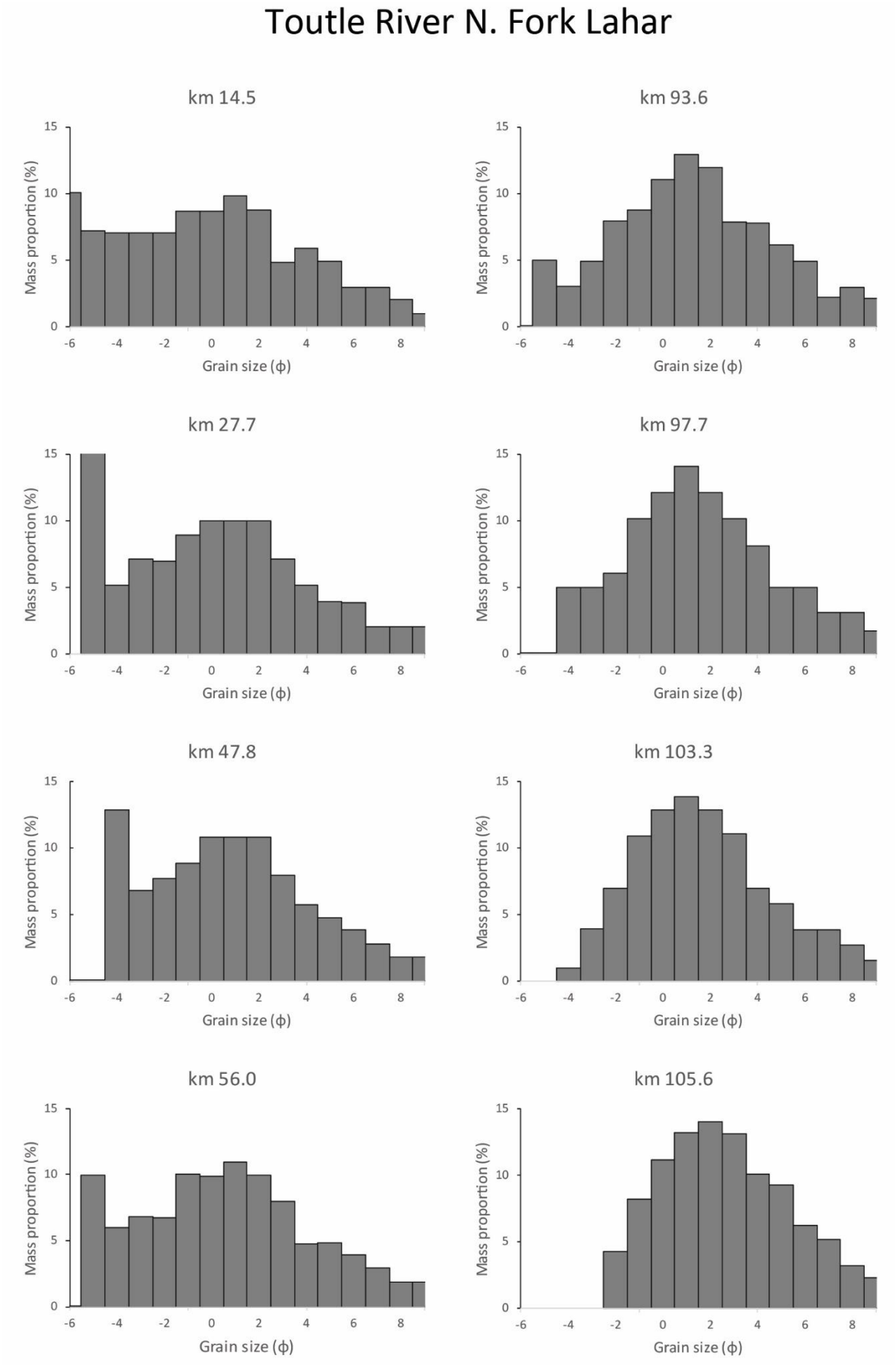
Toutle River N. Fork Lahar
km 14.5
km 93.6
km 27.7
km 97.7
km 47.8
km 103.3
km 56.0
km 105.6
Mass proportion (%)
Grain size (ϕ)
0
5
10
15
-6
-4
-2
0
2
4
6
8

Figure 8